Subvolt Broadband Lithium Niobate Modulators

M.M. Howerton, R.P. Moeller, and J.H. Cole
Optical Sciences Division

J. Niemel
SFA, Inc.

Introduction: Analog fiber-optic links have been extensively investigated for the transmission of radio frequency (RF) signals for military applications, including satellite communications systems and phased array antenna systems. This field is known as microwave photonics. Compared to coaxial cables, optical fibers offer immunity to electromagnetic interference and low propagation losses with nearly unlimited bandwidth. A basic fiber-optic link is composed of an optical source, an optical modulator that uses an electrical signal to modulate an optical signal, fiber for transmitting the modulated optical signal, and a photodetector. One key link parameter is conversion loss, which is a measure of the output RF power (optical power converted to electrical by the photodetector) to the input RF power at the modulator. It is important to minimize conversion loss. This can be done by using high-power lasers, modulators with low drive voltages, and sensitive photodetectors.[1]

The objective of this program is to develop optical waveguide modulators that achieve subvolt drive voltages to 20 GHz, with the intention of using the modulators in RF links to attain zero conversion loss. We use lithium niobate as the substrate material because it is a mature technology with good long-term stability, and it has a strong electrooptic coefficient that leads to low drive voltages. Other advantages are its low optical loss and its capability to operate at high frequencies. Lithium niobate modulators are available commercially and are used in optical communications systems. The technology we have developed at the Naval Research Laboratory has been at the leading edge of the field, and has resulted in record low drive voltages for high-speed packaged, lithium niobate modulators in a single-pass configuration (5 V at 40 GHz).[2] We have also demonstrated subvolt drive voltages in a reflection modulator to 0.5 GHz.[1] To achieve subvolt drive voltages to 20 GHz in the current program, we have developed a novel serpentine design that allows for very long interaction lengths.

High-Speed Modulator Operation: Figure 1 shows our conventional single-pass modulator, which is a Mach-Zehnder interferometer. The interferometer consists of optical waveguides that are photolithographically formed by titanium diffusion in lithium niobate, and overcoated with a silicon dioxide buffer layer and gold electrodes. Long interaction lengths help reduce the drive voltage V_π at dc, but at the same time demand low electrode losses to minimize the unavoidable increase in V_π with frequency. Very thick (20 to 30 μm) traveling wave electrodes are used to minimize electrode losses and to match the velocities of the microwave and optical signals, which is essential for broadband operation. We have recently developed the capability to form ion milled ridges in lithium niobate to impedance-match the modulator structure to the external microwave source, so the complete fabrication of the modulators is done in-house. Sophisticated computer modeling is used to select layer thicknesses and gap widths that result in optimal velocity and impedance matching while maintaining low electrode losses.

Figure 2 shows our new design for a traveling wave modulator that uses 180-deg turns to increase the interaction length. By using three passes, for example, the dc V_π is reduced by a factor of three. Since conventional semicircular turns require too much real estate (with bend diameters exceeding 2 cm for <1 dB loss), we are now developing a serpentine traveling wave modulator with low-loss compact turns in lithium niobate waveguides. The idea is to pack multiple passes on the same chip (6 cm long × 6 mm wide) that previously contained only one pass. We have successfully accomplished our goal of low-loss-compact turns by using a novel approach that consists of a reflective s-bend placed at the edge of the substrate. This extremely promising technique has resulted in losses as low as 0.6 dB, while simultaneously reducing lateral space requirements by over two orders of magnitude when compared to semicircular turns. A key fabrication issue is ensuring that the mirrored edge is within a few microns of the s-bend apex. Reflective s-bends are also an attractive technique for integrating different devices on the same chip.

Figure 3 is a model of drive voltage as a function of frequency from dc to 20 GHz for modulators with different interaction lengths at the 1.55 μm wavelength. The "previous" curve with 0.04 (GHz$^{1/2}$-cm)$^{-1}$ electrode loss corresponds to our recently published single-pass modulator. Current electrode loss has been improved to 0.025 (GHz$^{1/2}$-cm)$^{-1}$ by increasing electrode thickness and gap widths. Note that while drive voltages of the single-pass device are around 3 to 4 V at 20 GHz, we can now push V_π near and below 1 V with the three-pass and ten-pass modulators as long as the electrode losses are kept small.
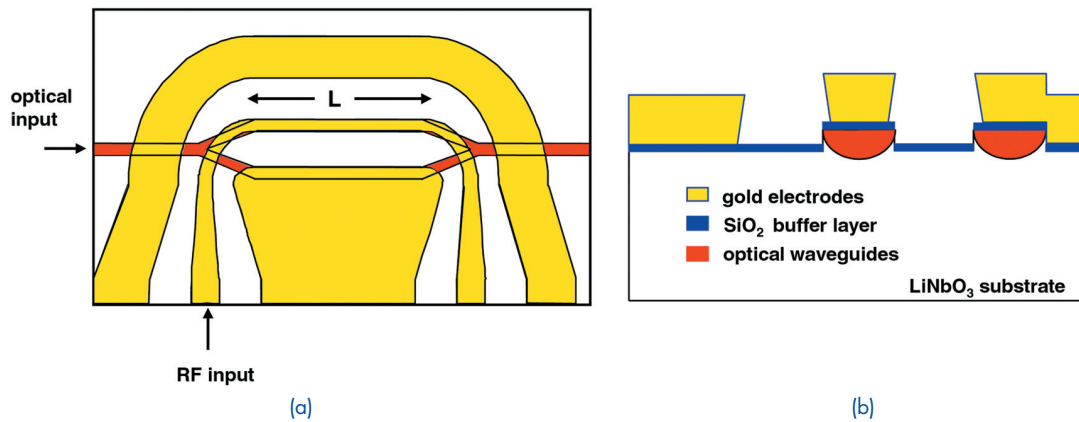
FIGURE 1
(a) Top view of a single-pass traveling wave modulator in lithium niobate with interaction length *L*; (b) Cross-section of interaction region.
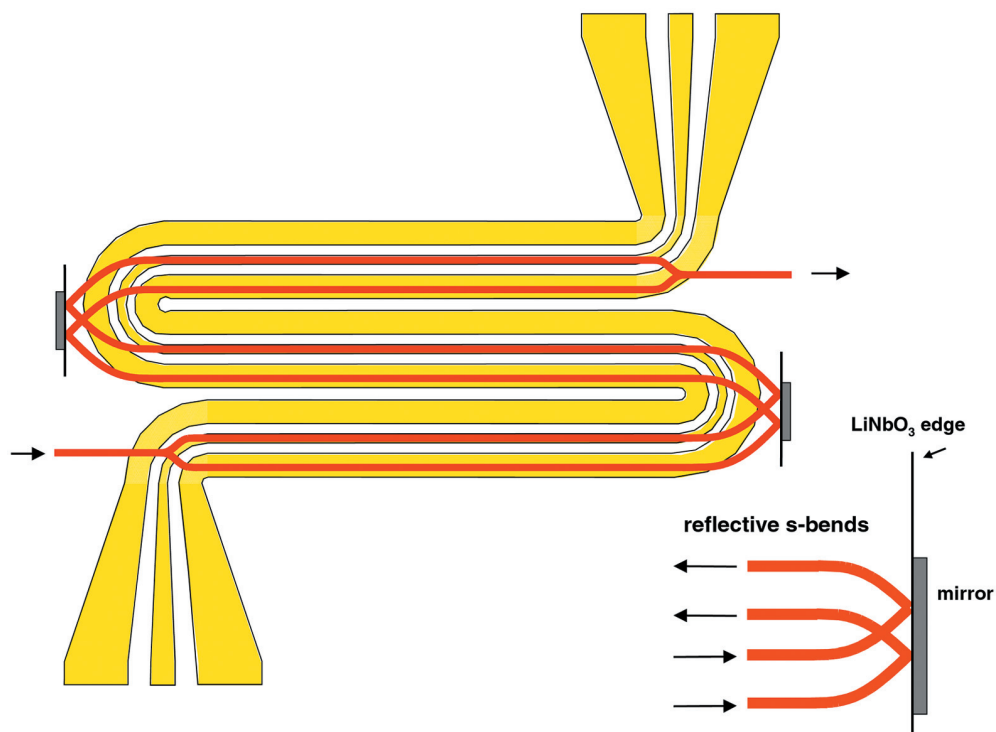

FIGURE 2
Schematic of the traveling wave serpentine modulator. The underlying waveguide layer is emphasized for clarity. Compact waveguide turns are formed by reflective *s*-bends at the lithium niobate edges, as shown in inset.
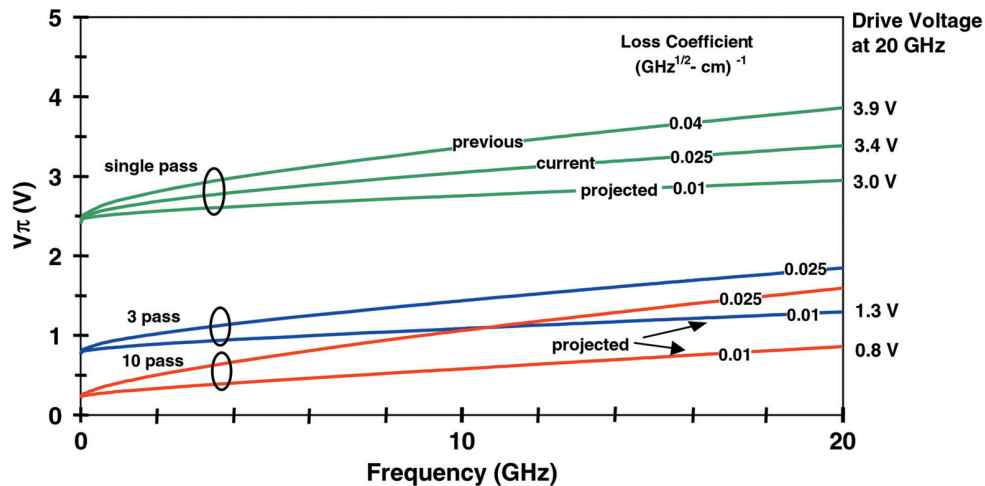
FIGURE 3
Drive voltage as a function of frequency for single-pass, three-pass, and ten-pass modulators, with electrode loss as a parameter.

Summary: We are developing broadband lithium niobate optical modulators designed to obtain subvolt drive voltages. Low drive voltage, high-speed modulation is achieved with traveling wave electrodes having a serpentine design, along with novel reflective *s*-bends that increase the interaction length.

[Sponsored by DARPA]

References
[1] W.K. Burns, M.M. Howerton, and R.P. Moeller, "Broad-band Unamplified Optical Link with RF Gain Using a LiNbO$_3$ Modulator," *IEEE Photon. Technol. Lett.* **11**, 1656-1658 (1999).
[2] M.M. Howerton, R.P. Moeller, A.S. Greenblatt, and R. Krähenbühl, "Fully Packaged Broad-band LiNbO$_3$ Modulator with Low Drive Voltage," *IEEE Photon. Technol. Lett.* **12**, 792-794 (2000). ■

Technology Demonstration of SHARP, the Navy's Next-Generation Tactical Reconnaissance System

M.D. Duncan, M.R. Kruer, D.C. Linne von Berg, and J.N. Lee
Optical Sciences Division

Introduction: The NRL Optical Sciences Division has designed, implemented, and demonstrated the prototype version of the SHAred Reconnaissance Pod (SHARP). The August 28, 2001 demonstration at the Pentagon showed successful operation of all aspects of a state-of-the-art, tactical digital reconnaissance system. This included dual-band visible and infrared (IR) imagery collection aboard both the Navy's F/A-18 Super Hornet aircraft and an NRL P-3, and downlinking the collected imagery in real time on a 274 megabit-per-second common data link (CDL) to the NAVy Input Station (NAVIS) ground station for real-time image screening and exploitation. Two cameras for standoff oblique imagery were demonstrated: one for medium range (approximately 5 to 15 nmi) and one for long range (approximately 15 to 50 nmi) on the F/A-18 and the P-3 aircraft, respectively. Technologies for in-cockpit image screening of reconnaissance imagery and for real-time nonuniformity correction of IR imagery were also demonstrated on the ground in conjunction with the airborne demonstration. The demonstration has had major impact; both Pentagon Tri-Service staff and Congressional staff were in attendance.

SHARP Hardware: Figure 4 shows the SHARP pod and payload. The SHARP pod, manufactured by Raytheon Technical Services Company (RTSC), is approximately the size of a 330-gal fuel tank and is carried on the centerline of an F/A-18 aircraft. The pod has a rotating midsection that keeps the pod's 11 × 18 in. window aligned with the camera optics. The pod also has an environmental control system designed to cool pod electronics. Visible and IR images captured by the camera are compressed, stored on a digital recorder, and simultaneously transmitted to the ground using a steerable antenna. The camera produces downsampled images that are sent as a video signal to the F/A-18 cockpit for aircrew monitoring. The F/A-18 crew can control the col-
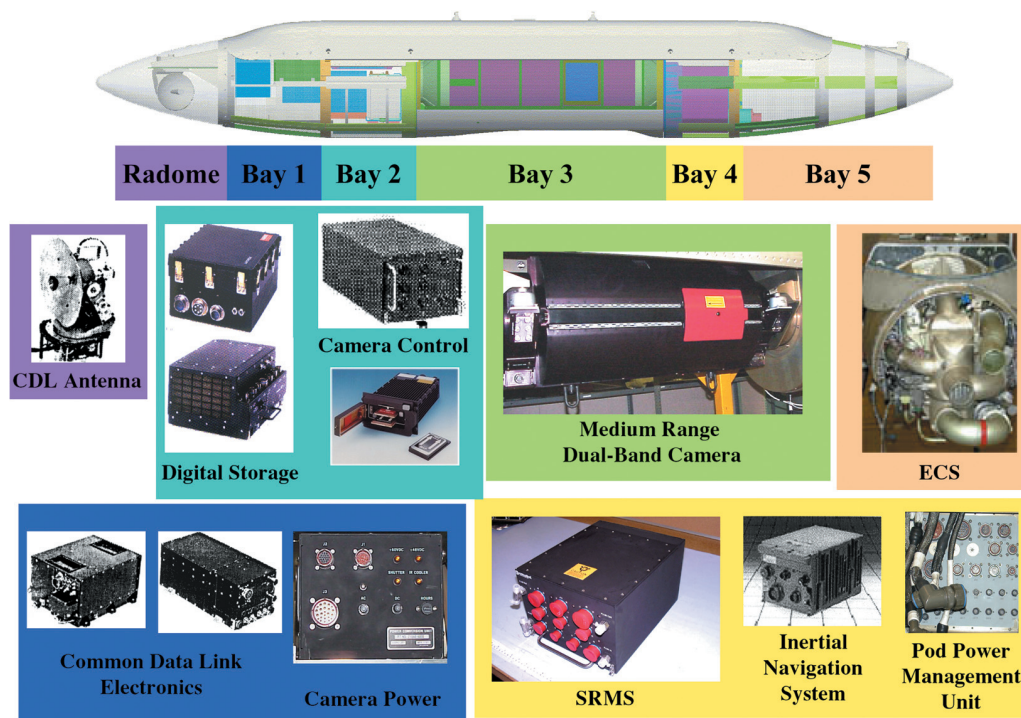
179

FIGURE 4
The SHAred Reconnaissance Pod (SHARP). Various electronic boxes that constitute the pod payload are shown, color coded to indicate the pod bay they are housed in.

lection, storage, and datalinking of reconnaissance data or those tasks can be completely automated using mission planning data.

NRL developed the hardware and software that constitutes the prototype SHARP Reconnaissance Management System (SRMS). This includes compression hardware (to reduce data-flow and data-storage requirements by >80%), control software for the camera and all other electronic components, and software for communicating with the aircraft. The prototype SHARP system was integrated, under NRL's direction, with the F/A-18 aircraft first at the Boeing Corporation in St. Louis, Missouri, and then at the Naval Air Warfare Center Weapons Division, China Lake, California, and Naval Air Warfare Center Aircraft Division, Patuxent River, Maryland. The SHARP payload was integrated with the SHARP pod at RTSC in Indianapolis, Indiana, and the completed pod underwent extensive testing there.

Simultaneous with the SHARP pod integration of the medium-range dual-band camera and the pod with the F/A-18 aircraft, NRL also directed the integration of a second set of SHARP electronics on an NRL P-3 aircraft. The second SHARP system was used to demonstrate a long-range camera during the Pentagon demonstration.

Figure 5 shows the SHARP pod on an F/A-18 aircraft. Figure 5(a) shows the F/A-18 on the ground, and Fig. 5(b) shows the same F/A-18 in flight over the Washington, D.C. area. During image acquisition, the pod midsection rotates the window to an operational position. The pod window can be seen in Fig. 5(b). Figure 5(c) shows an NRL P-3 with a modified bomb-bay structure for supporting a camera and window. Figure 5(d) shows a close-up of the camera support structure.

Test and Demonstration Flight Results: The two cameras flown during the SHARP demonstration were first evaluated for technical maturity on an NRL P-3. Figure 6 shows images of the Washington, D.C. area taken with the medium-range CA-270 camera on December 20, 2000. Both visible (Fig. 6(a)) and IR (Fig 6(b)) images were taken simultaneously at an altitude of 11,000 ft. The slant-range distance from the P-3 to the ground was 5.4 nmi for the near edge of the pictures and 10.2 nmi for the far edge. The visible image size is 5040×5040 pixels and the IR image size is 1680×1680 pixels.

Figure 7 is the waterfall display that was received over the datalink by the NAVIS ground station during the August 28, 2001, Pentagon demonstration

(a)

(b)

(c)

(d)

FIGURE 5
The F/A-18 and P-3 aircraft that carried the SHARP payloads. (a) The F/A-18 with the SHARP pod on the ground. The SHARP pod is carried on the centerline of the aircraft. (b) The F/A-18 with the SHARP pod flying over Washington, D.C. Note the pod window. (c) The NRL P-3 that also carried the SHARP payload. (d) A close-up view of the camera support structure and window on the P-3.

(a) Visible image

(b) IR image

FIGURE 6
Images taken by a CA-270 dual-band, medium-range camera of the Washington, D.C., area on December 20, 2000. The P-3 altitude was 11,000 ft for these images.
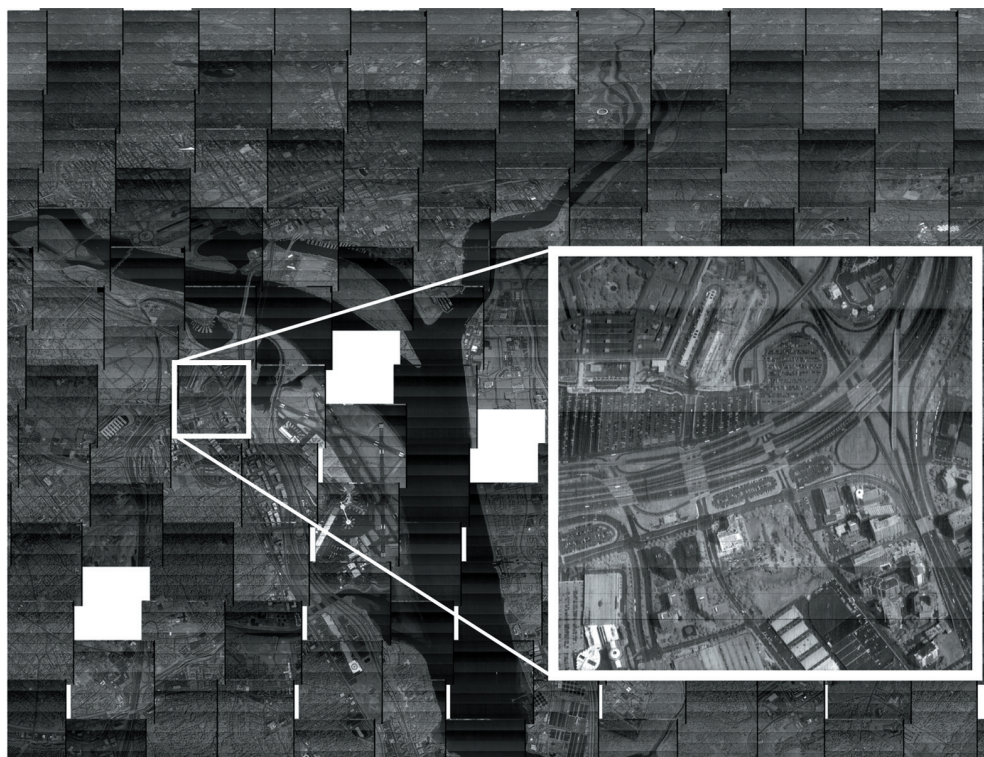
FIGURE 7
A mosaic of images as received on the NAVIS ground station during the Pentagon demonstration on August 28, 2001. Each downsampled image can be clicked on to produce a full-resolution image, as shown in the inset.

flight. The data are from the medium-range camera flown on the F/A-18 aircraft. The mosaic of images is created from the downsampled images produced by the camera as it rotates in the cross-flight direction and takes a swath of snapshot images. The images are placed in their proper position geographically in real time using navigation data from the pod and aircraft. The full-resolution images are also received in real time, and they are available instantaneously when the NAVIS user clicks with a mouse on a downsampled image. The exploded view in Fig. 7 is a single full-resolution image showing part of the Pentagon in the upper left-hand corner. Combined with the aircraft navigational data, the NAVIS ground station provides accurate geolocation and mensuration capabilities on the full-resolution images. When combined with *Falcon View* flight planning software, a moving-map display of the sensor platform and camera coverage can also be displayed, as shown during the Pentagon demonstration.

Future tactical reconnaissance capabilities will depend on shortening the time between target detection and target strike. NRL has developed and demonstrated the Airborne Real-time Imagery Exploitation System (ARIES), a single board processor suitable for incorporation into the SRMS that provides the flight crew with enhanced image exploitation capability for time-critical strike. ARIES was operated on the ground at the Pentagon demonstration.

Conclusions: SHARP is scheduled to replace the Navy's current F-14 film reconnaissance capability by January 2003. Because of this tight schedule, the prototype phase of the SHARP program was established to demonstrate the maturity of new technical capabilities and to reduce the technology risk to later phases of the SHARP program. The prototype program successfully demonstrated real-time reconnaissance operation of the prototype SHARP system on an F/A-18 and of the prototype SHARP payload on a P-3 in coordinated flights. Each aircraft downlinked imagery to a NAVIS ground station and displayed that imagery in real time to the audience on August 28, 2001. The principal technology objectives—to verify that dual-band camera technology was sufficiently mature, and that the SRMS with its operating software could control the SHARP subsystems and deliver real-time high-bandwidth reconnaissance imagery—were achieved through the demonstration flight. The prototype system is now used as a test asset in support of the SHARP program.

[Sponsored by ONR] ■

Photonic Ultrawideband Millimeter Wave Beamformer

D.A. Tulchinsky
Optical Sciences Division

Introduction: Electronically steered radar systems are currently used in a variety of military and commercial applications. The speed and agility of electronically steered beams is far superior to those from mechanical steered antennas. These applications include electronic countermeasure and surveillance radars, Improving array systems to transmit and/or receive across an ultrawide frequency bandwidth (percentage bandwidths greater than 25%) would upgrade high-resolution mapping/target identification radar systems. Furthermore, the military currently needs radar systems capable of operating within the millimeter wave (MMW) frequency range (30 to 300 GHz). Trying to satisfy all these performance goals has historically proved to be a significant challenge. For example, the development of MMW radar systems has been slowed because of the lack of high-power sources and low-loss millimeter wave components. Current electronically steered systems normally have narrow bandwidths (percentage bandwidths less than 1%) for reasons of cost and performance.

Array antennas are steered by delaying the RF signal at each antenna feed by an appropriate amount of time (Fig. 8). When the radiated waves combine, constructive interference occurs and the signal power adds in the desired pointing direction, forming the main beam. In narrowband systems, these time shifts are produced using RF phase shifters. However, ph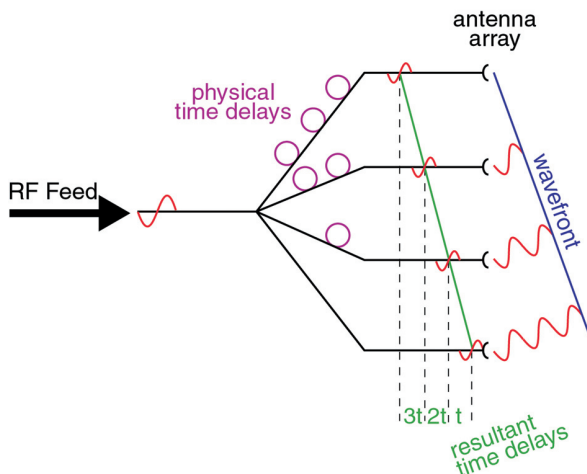ase shifters are not suitable for ultrawideband systems because phase control is not capable of steering wide frequency bandwidths to the same point in space. Hence, ultrawideband systems require true-time delay (TTD) techniques to avoid frequency-dependent steering effects. The Optical Science Division of NRL has developed a fiber-optic beamforming system that implements TTD.[1] In this article, we show that this photonic TTD architecture is extendable into the MMW frequency range and is capable of steering ultrawideband arrays.[2]

Beamformer Design: Figure 9 is a schematic of the photonic millimeter wave beamformer. A wavelength tunable semiconductor laser serves as the optical source for the system, after which an erbium-doped fiber amplifier (EDFA) boosts the laser's output power. Optical fiber directs the light into a 40 GHz electro-optic Mach-Zehnder intensity modulator (MZM). The MZM takes the input RF signal and impresses its signature onto the amplitude of the light. The modulated optical signal is fed into a four-channel fiber-optic dispersive prism. The optical dispersion gradient in the dispersive prism translates a wavelength change of the laser into an optical path length difference among the prism's channels. This change in path length provides the time-delays between the prism's four output channels that are required to steer the RF beam. After the prism, the four optical paths continue through separate fiber-optic length and amplitude trimmers (not shown) before being directed onto the photodetectors. The photodetectors, sensitive to modulations in optical power up to 50 GHz, convert the optical signals into RF electrical signals—replicas of the input RF signal. Each resulting RF path is amplified by a low-noise MMW amplifier and fed into the input plane of a MMW antenna array.

Demonstration and Results: After construction and testing in the laboratory, further experiments on the photonic beamformer were performed in a MMW anechoic radar range within the Tactical Electronic Warfare Division's Radar Range Facilities. In the range, the beamforming system is mounted on a multi-axis positioning stage, and the RF radiation from the transmitting antenna array is focused onto a receive antenna by an off-axis parabolic microwave mirror. While the positioner rotates the photonic beamformer in the azimuthal direction through a ±70° sweep, a microwave network analyzer records the frequency response of the system between 20 and 45 GHz in the forward-looking direction.

Figure 10 shows examples of the transmitted intensity patterns with the laser tuned to steer the beam to −15°, 0°, and +30° away from the forward looking direction for frequencies across the entire

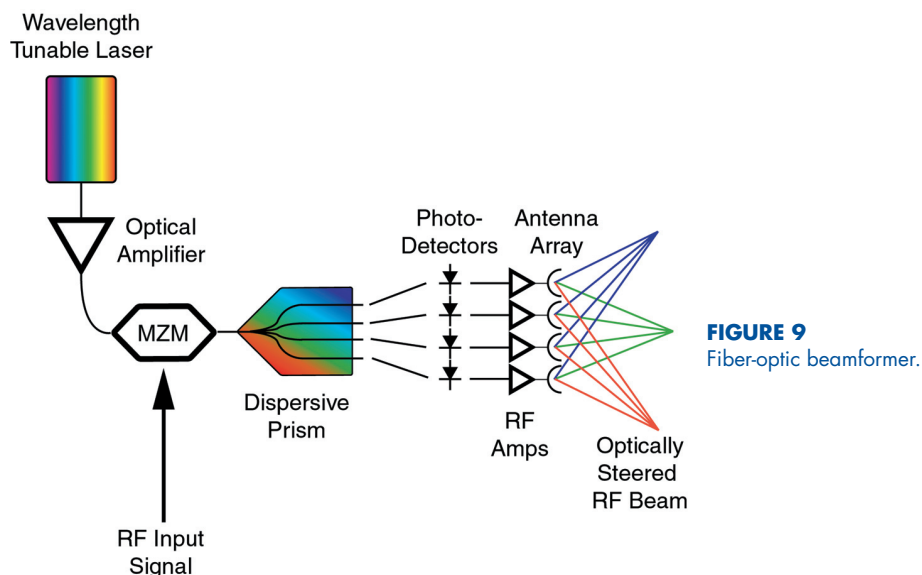**FIGURE 8**
True time-delay beam steering.
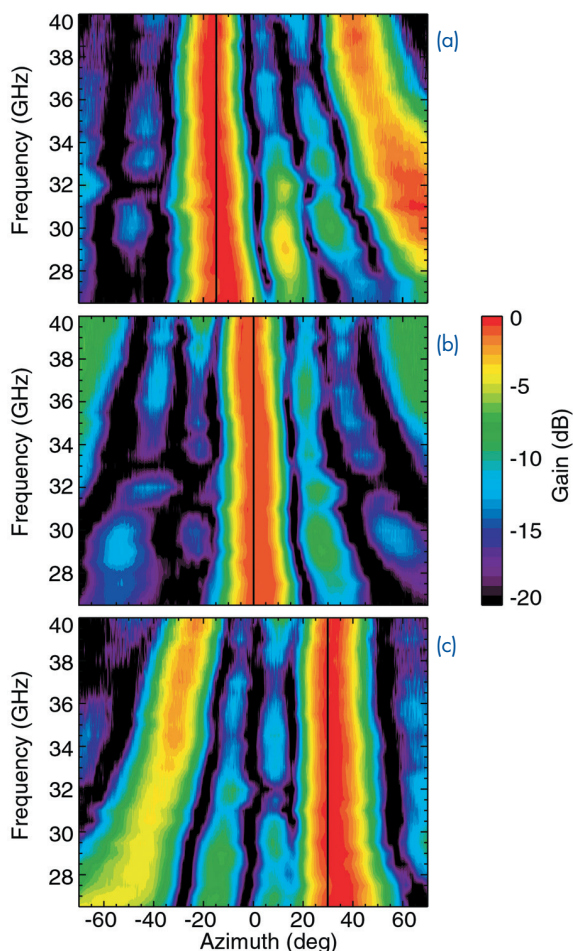
FIGURE 9
Fiber-optic beamformer.

FIGURE 10
Transmitted intensity plot as a function of mechanical angle and frequency with the laser adjusted for optical steering to (a) −15°, (b) 0°, and (c) 30° in azimuth. The black vertical lines are guides to the eye to indicate at what azimuthal angle the beam is steered.

Ka (26.5 to 40 GHz) frequency band. These intensity plots show that the main intensity of the transmitted RF beam is at the expected steered angle and the steering is independent of frequency. On either side of the mainbeam lobe, RF intensity is expected and present in two beam sidelobes as well as one grating lobe. Note how the sidelobes and the grating lobes exhibit the expected frequency-dependent steering.

Summary: NRL has successfully demonstrated a photonically controlled ultrawideband beamformer for millimeter wave transmit arrays. The high speed and large bandwidth potential of photonics make this system an attractive alternative to conventional array beamformers.

References
[1] R.D. Esman, M.Y. Frankel, J.L. Dexter, L. Goldberg, M.G. Parent, D. Stilwell, and D.G. Cooper, "Fiber-optic Prism True Time-delay Antenna Feed," *IEEE Photon. Technol. Lett.* **5**, 1347 (1993).
[2] D.A. Tulchinsky and P.J. Matthews, "Ultrawide-Band Fiber-Optic Control of a Millimeter-Wave Transmit Beamformer," *IEEE Trans. Microwave Theory Tech* **49**, 1248 (2001). ■